LASER INTERFEROMETER GRAVITATIONAL WAVE OBSERVATORY

LIGO Laboratory / LIGO Scientific Collaboration

LIGO-T0900407-v4 *ADVANCED LIGO* 01/11/10

Pre Mode Matching Telescope Parameters, Adaptive Mode matching, and Diagnostics

Muzammil A. Arain, Luke F. Williams, Guido Mueller, and David H. Reitze

Distribution of this document:
LIGO Science Collaboration

This is an internal working note
of the LIGO Project.

California Institute of Technology
LIGO Project – MS 18-34
1200 E. California Blvd.
Pasadena, CA 91125
Phone (626) 395-2129
Fax (626) 304-9834
E-mail: info@ligo.caltech,edu

Massachusetts Institute of Technology
MIT NW22-295
185 Albany Street
Cambridge, MA 02139 USA
Phone (617) 253-4824
Fax (617) 253-7014
E-mail: info@ligo.mit.edu

LIGO Hanford Observatory
P.O. Box 1970
Mail Stop S9-02
Richland WA 99352
Phone 509-372-8106
Fax 509-372-8137

LIGO Livingston Observatory
P.O. Box 940
Livingston, LA 70754
Phone 225-686-3100
Fax 225-686-7189

http://www.ligo.caltech.edu/

1 Introduction

1.1 Purpose and Scope

This document describes the optical parameters and the layout for the pre mode matching telescope for the Advanced LIGO cavities in HAM2/HAM8. We also describe the diagnostics for the mode matching and adaptive mode matching operation.

1.2 Definitions

Finesse: Measure of the selectiveness/build-up of a cavity given by $F = \frac{\pi\sqrt{r_1 r_2}}{1 - r_1 r_2}$

Free Spectral Range: The FSR = $\frac{c}{2\mathrm{L}}$ where c is the speed of light while L is the length of the cavity. The units we use are Hz.

Linewidth: The frequency at which the normalized transmission through a cavity drops to 0.5. Linewidth = $\frac{0.5 * FSR}{F}$ = Half-Width-Half-Max (HWHM).

Transversal Mode Spacing: Transversal mode spacing is the frequency difference between two Gaussian modes with a differential mode index of 1. For example, this is the frequency difference between TEM_{00} mode and TEM_{01}. For any higher order TEMnm mode, the difference between TEMoo and TEMnm mode is given by $\frac{(n+m)FSR * a\cos(\pm\sqrt{g})}{\pi}$ where g is the G-factor of the cavity. Note that we will use Hz as the units of transversal mode spacing.

Sagitta or Sag: The sagitta of the wavefront of a beam measured between the center and at a radial distance equal to the 1/e beam radius w. Or the sagitta of a curved mirror with radius of curvature R measured over a radial distance of the expected beam radius w. The sagitta is equal to $\frac{w^2}{2\mathrm{R}}$.

1.3 Acronyms

AOE: Adaptive optical element
ROC: Radius of curvature
PRC: Power recycling cavity
PRM: Power recycling mirror
RC: Recycling cavity
SRC: Signal recycling cavity
IMC: Input mode cleaner
PMMT: Pre-mode matching telescope
BSS: Beam Size Sensor

1.3.1 LIGO Documents

1. Michael Smith and Dennis Coyne, “Stable Recycling Cavity Mirror Coordinates and Recycling Cavity Lengths,” LIGO-T080078-06-D.
2. Muzammil A. Arain and Guido Muller, “Design of the Advanced LIGO recycling cavities,” Opt. Express 16, 10018-10032 (2008) http://www.opticsinfobase.org/abstract.cfm?URI=oe-16-14-10018.

3. R. Abbott et al., "Advanced LIGO Interferometer Sensing and Control Conceptual Design," LIGO-T070247-00-I.
4. Muzammil A. Arain and Guido Muller, "Optical Layout and Parameters for the Advanced LIGO Cavities," LIGO Technical Note, https://dcc.ligo.org/public/0000/T0900043/005/LIGO-T0900043-08.pdf, (look for the latest document version).
5. Luke F. Williams, LHO Layout, LIGO Drawing LIGO-D0900888.
6. Luke F. Williams, LLO Layout, LIGO Drawing LIGO-D0900919.
7. Muzammil A. Arain, "A Note on Substrate Thermal Lensing in Mode Cleaner," LIGO Technical Note LIGO-T LIGO- T070095-00-E, http://www.ligo.caltech.edu/docs/T/T070095-00.pdf .
8. Muzammil Arain et al., "Adaptive control of modal properties of optical beams using photothermal effects," Manuscript in preparation, LIGO DCC document LIGO-P0900116 available at https://dcc.ligo.org/cgi-bin/private/DocDB/ShowDocument?docid=5996.
1. Muzammil A. Arain, David H. Reitze, "Engineering Specifications of adaptive ring heater in IO for Advanced LIGO," LIGO DCC document LIGO-E0900268, available at (look for the latest document revision).

2 Optical Configuration

The optical configuration of the Advanced LIGO cavities is given in Fig. 1 where we include both recycling cavities and the arm cavities.

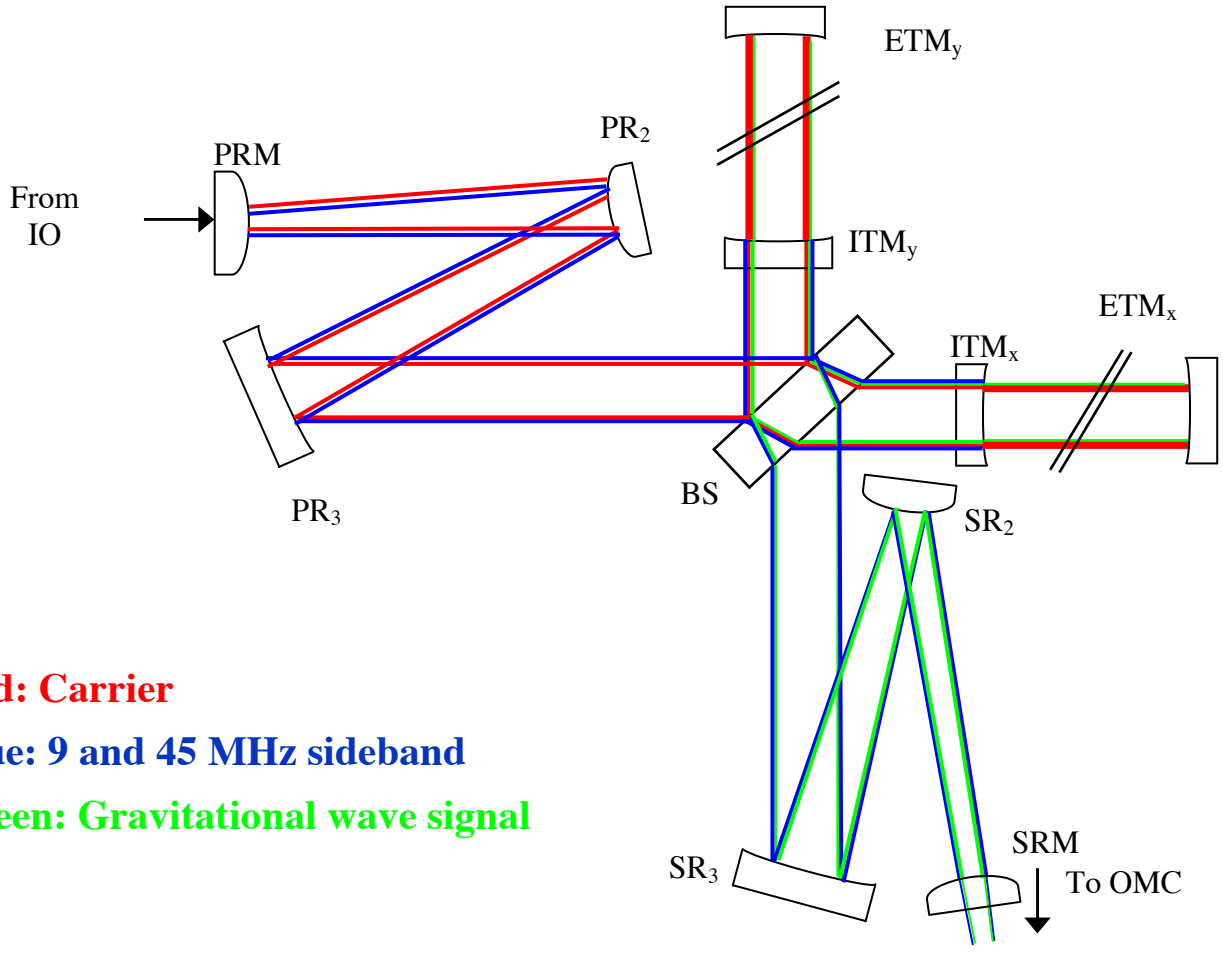

Fig. 1: Optical layout of Advanced LIGO cavities.

The proposal to incorporate stable recycling cavities in Advanced LIGO has been adopted as the base-line design for Advanced LIGO.[1] The lengths of the cavities have been selected and described in Ref. 2 and 3. These lengths constraints and the choice of specific Gouy phases [1,4] require extra mode matching between the mode cleaner (IMC) and the interferometer. Therefore, the beam from the IMC has to be shaped properly to match the beam size and ROC required at the PRM. The conceptual layout of the pre-mode matching telescope is shown in Fig. 2.

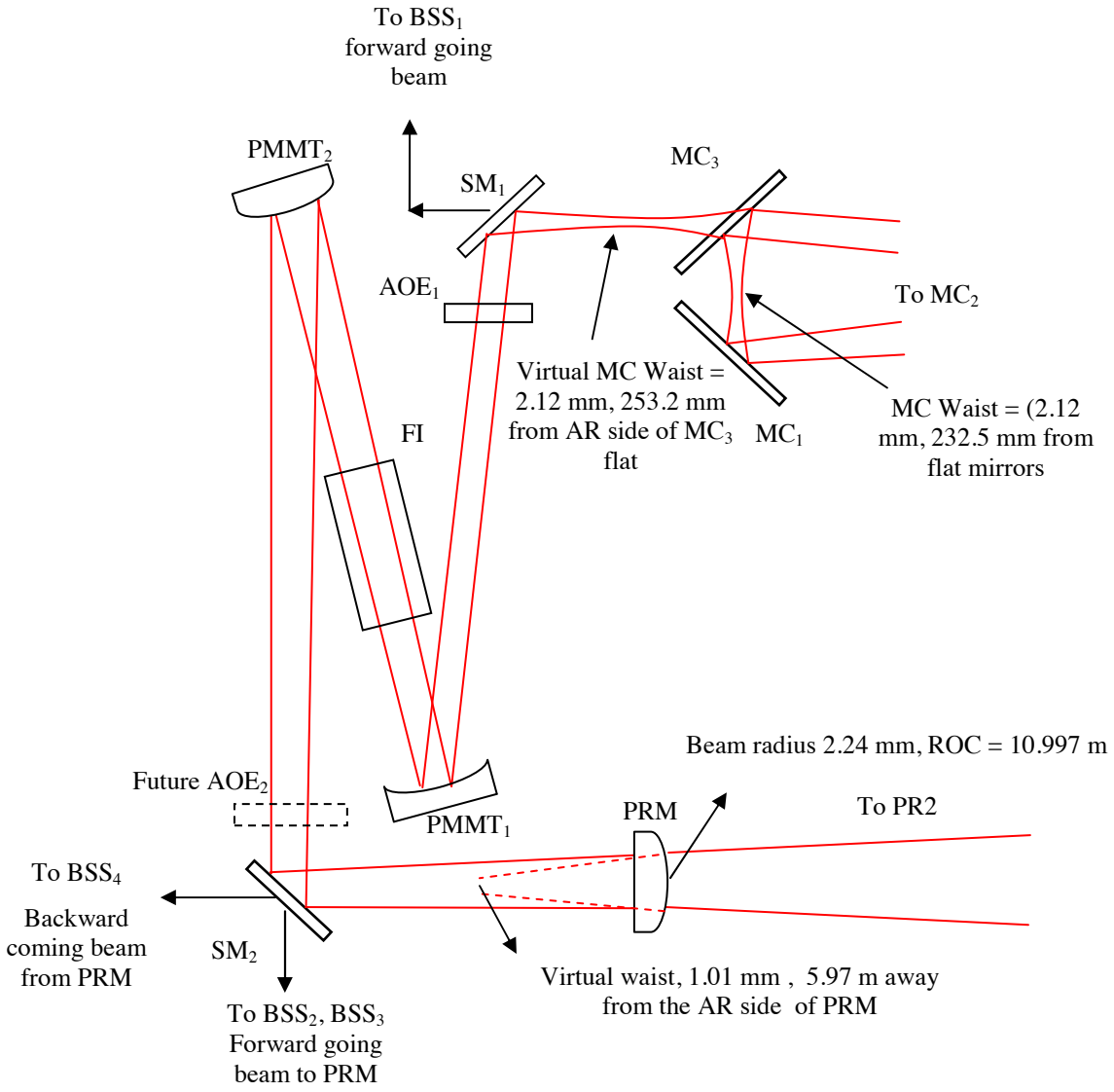

Fig. 2: Optical Layout of HAM2 Table including details of PMMT for the H1 and L1 interferometers. The numbers shown are for straight interferometers. AOE stands for Adaptive Optical Element. Folded interferometer numbers are included in Appendix A. The detailed layout drawings are shown in Ref. 5 and 6.

---

[1] Michael Smith and Dennis Coyne, "Stable Recycling Cavity Mirror Coordinates and Recycling Cavity Lengths," LIGO-T080078-06-D.

2.1 ROC Sensitivity of PMMTs

Fig. 3 shows the mode matching between the IMC mode and the straight and folded interferometers PRC mode (where 1.0 = perfect mode matching) as a function of the ROC of the $PMMT_1$ mirrors (normalized to their design value) for different $PMMT_2$ ROCs. Although the plot is generated with large tolerances, the design tolerances for the ROCs of these mirrors are 1%. For these values, the mode mismatch is well below 0.2%.

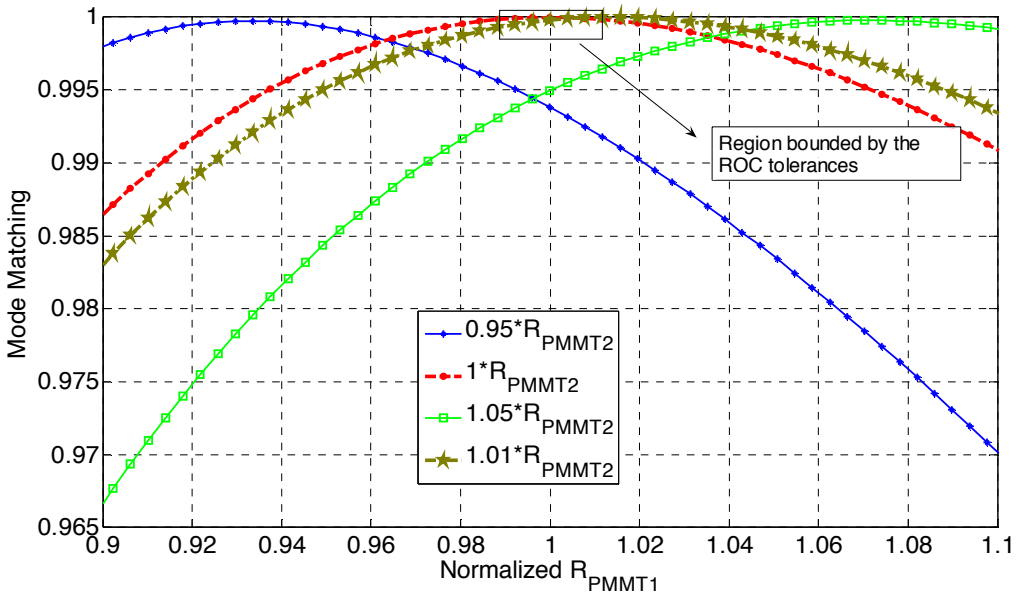

(a)

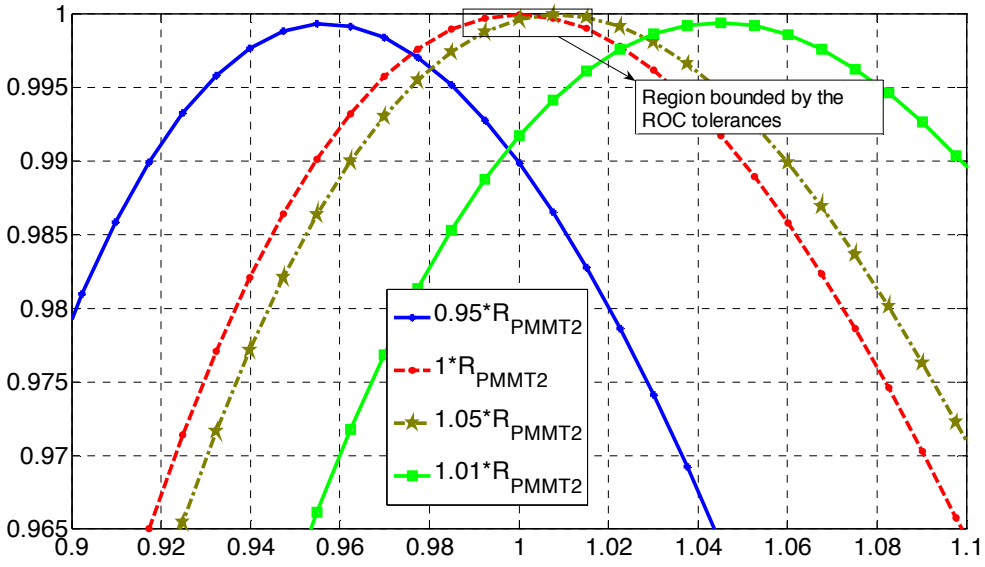

(b)

Fig. 3: Mode matching as a function of normalized $PMMT_1$ ROC for the a) straight and b) folded interferometer. Curves are shown for select values of the $PMMT_2$ ROC with $PMMT_1$ ROC as variable. A small rectangular box shows the range of mode mismatch that is expected for the given ROC tolerances. The mode matching is hardly affected by the given range.

Note that Fig. 3b shows more sensitivity to mode mismatches. This is due to the fact that the PMMTs in the folded interferometer have relatively stronger ROCs as compared to the straight folded interferometer.

2.2 Displacement Sensitivity

The PMMT forms a very slow telescope. There is no beam waist between the PMMT mirrors and the beam waist is well outside the Rayleigh range. The ROC values of the PMMT mirrors are relatively large with the smallest being -3 m in the folded design. Therefore, as is evident from section 2.1, the telescope is very insensitive to ROC errors. In a similar fashion, the telescope is quite insensisitive to positioning errors as well. This behavior is shown in Fig. 4.

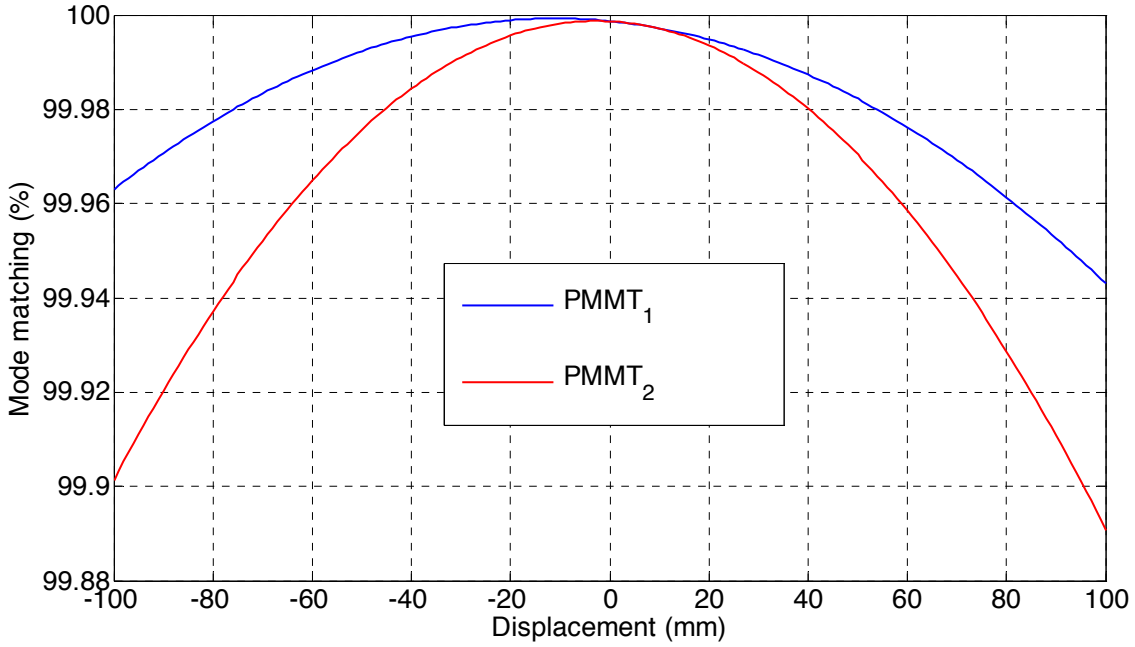

Fig. 4: Mode matching as a function of positioning error for $PMMT_1$ and $PMMT_2$ mirror for the straight interfeorometer shown as displacement from the designed value.

3 Mode Mismatch Analysis

Mode mismatch between the input beam and the interferometer eigenmode at the PRM can be caused by ROC mismatches and by beam size mismatches. Any optical component within the input optics acts only on the ROC of the beam. This will then change the beam size downstream. A change in the ROC at one location will turn into a pure beam size change after the mode accumulates a 45deg Gouy phase.

Fig. 5 presents the beam size evolution and accumulated Guoy phase from the IMC waist to the PRM for the straight and the folded interferometer. The total Gouy phase of the system is around 20 degree. Consequently, a change in the beam size along the optical path between the IMC and the

PRM is virtually impossible to compensate. However, as we will show in the next subsections, a direct change of the beam size is very unlikely while changes in the ROC of the phase front can be corrected at or near the component which causes the change leaving the beam size unaffected.

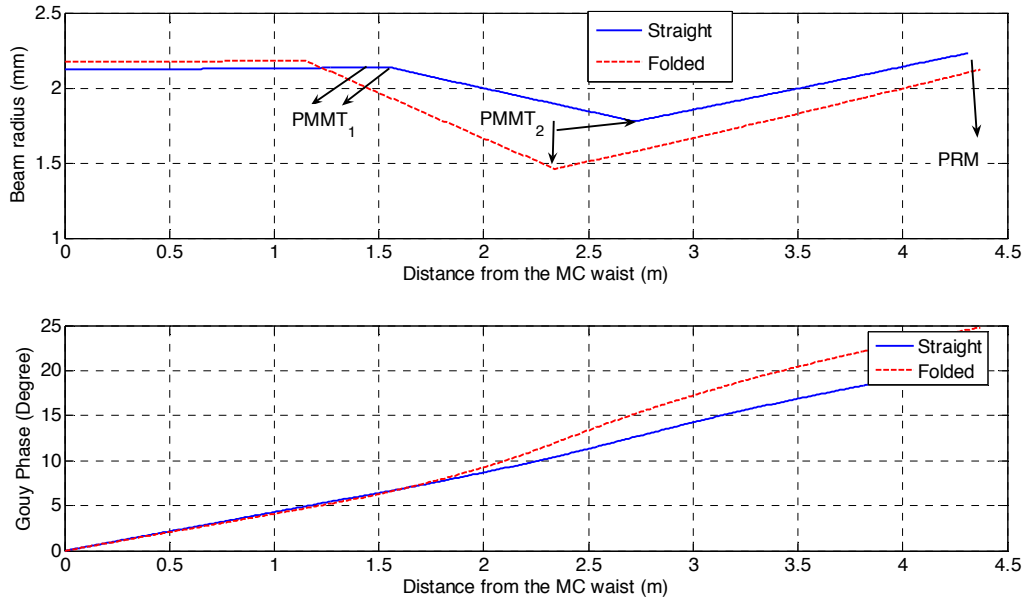

Fig. 5: Beam size change and Gouy phase change in the straight and folded interferometer

4 Sources of Mode Mismatch

4.1.1 Beam Size Mismatch

The input beam size for the mode matching between the IMC and the IFO is the beam waist of the mode cleaner Eigenmode. This Eigenmode depends upon the ROC of the curved mirror and any surface thermal lensing in the flat mirrors. The tolerances of the ROCs of all three mirrors were derived such that the mode matching between the IMC and the main interferometer is above **99%**. It has been shown that the surface thermal lensing in the IMC is expected to be very small in Advanced LIGO.[2] Fig. 6 shows the IMC mode change versus IMC input power assuming 0.5 ppm coating absorption. Hence the changes in the IMC eigenmode inside the IMC will be minimal and don't require any compensation. This does not include the thermal lens induced by the substrate of the IMC output mirror (see next section).

[2] Muzammil A. Arain, "A Note on Substrate Thermal Lensing in Mode Cleaner," LIGO Technical Note LIGO-T LIGO- T070095-00-E, http://www.ligo.caltech.edu/docs/T/T070095-00.pdf .

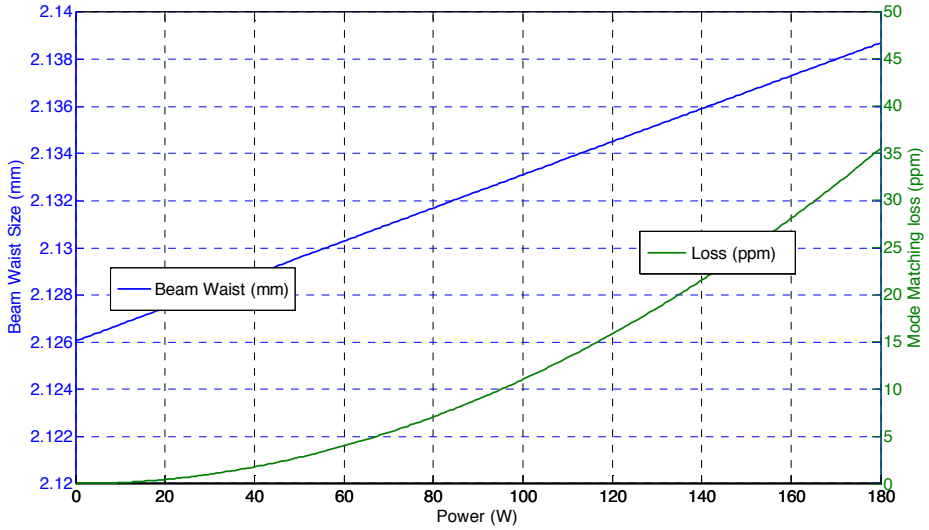

Fig. 6: Beam waist size variation due to combined effect of 0.5 ppm absorption of IMC mirrors (surface thermal lensing). The corresponding power loss in the mode matching is plotted on right y-axis.

4.1.2 Beam ROC Mismatch

There are a number of sources that can change the ROC of the input beam:

1. IMC Substrate thermal lensing in IMC_3
2. $PMMT_1$ ROC tolerance or positioning error
3. FI thermal compensation
4. $PMMT_2$ ROC tolerance or positioning error

Out of these, we showed that the ROC tolerances or positioning errors in the PMMT are not significant. Thus the remaining ROC mismatch sources are IMC substrate thermal lensing and FI thermal lensing.

FI thermal lensing has been described in detail elsewhere[3] and the current ELIGO FI shows that the thermal lensing can be significantly reduced using a passive compensation system based on a matched DKDP crystal. However, the differences in the lab conditions and the HAM conditions make it difficult to optimize the compensation system to a degree consistent with the mode matching goals. The IMC substrate thermal lensing is expected to be small but it could be astigmatic[4].

[3] Muzammil A. Arain, "A note on A Note on Substrate Thermal Lensing in Mode Cleaner," LIGO Technical Note LIGO-T LIGO- T070095-00-E, http://www.ligo.caltech.edu/docs/T/T070095-00.pdf .

We propose to use adaptive compensation in the form of an adaptive optical element (AOE) to correct for the remaining ROC errors caused in the FI and the IMC. This system is described in detail in Ref. 8 and 9 while the next section discusses the range and location of the AOE.

5 Adaptive Mode Matching

The adaptive optical element (AOE) can produce a negative thermal lense to compensate the positive lenses induced in most of our components. The only other system element which creates a negative thermal lens is the DKDP crystal used to compensate the thermal lens in the TGG crystal of the FI. The expected thermal lens focal length depends on the residual absorption in the TGG crystal but should not be shorter than 10 m in each crystal. The thickness of the DKDP crystal will be chosen to compensate most of the thermal lens in the TGG crystal without overcompensating it. The remaining lens will be well above 50 m. The dynamic range of the AOE is about -10 m. Therefore, we have sufficient range to compensate FI and IMC thermal lensing.

5.1 Number of Adaptive Optical Elements

In the ideal case, we need two AOEs to compensate mode matching errors. These AOEs should ideally be 90^0 Gouy phase apart for orthogonal operation. However, the total Gouy phase between the IMC and the PRM is 20^0. Therefore, one AOE placed between the IMC and the FI should be sufficient to compensate the mode mismatching induced by both elements. Therefore, we will put one AOE in the system next to SM1.

5.2 Provision for Two AOEs

As stated earlier, IO is responsible to provide mode matching to the cold interferometer state. The cold sate is defined by the bean size and the ROC at the PRM. However, there may be certain scenarios where the mode at the PRM may change due to imperfect TCS or higher than expected thermal lensing in the IFO. For such cases, it will be advantageous to have two control knobs in the IO chain. This will provide double the dynamic range of one AOE and some degree of non-degeneracy (due to limited Gouy phase) in the IO chain. Since putting two AOE is not the base-line design, we do not provide details of how to incorporate two AOEs for compatible operation with IFO. However, there is space in HAM2/8 for a second AOE element following the FI and $PMMT_2$.

6 Mode Matching Diagnostics

6.1 IO-COC Interface

The IO responsibility is to provide a beam at the PRM interface with the right beam size and ROC. which matches the eigenmode of the cold interferometer. [4]

[4] Muzammil A. Arain and Guido Muller, "Optical Layout and Parameters for the Advanced LIGO Cavities," LIGO Technical Note, https://dcc.ligo.org/public/0000/T0900043/005/LIGO-T0900043-08.pdf, (look for the latest document version).

6.2 Strategy to ensure Mode-matching

We use beam size measurements via CCD camera to measure the modal profile of the beam at various locations. We use four beams to monitor and diagnose mode matching. The purpose and scope of these sensors is described below. The location of these sensors is shown in Fig. 2 as BSS_1, BSS_2, BSS_3 and BSS_4. All cameras will be Gigabit Ethernet (GigE) camera. We plan to use GC-1380 GigE cameras with a 2/3" size from Prosilica.

Figure **7** shows the location of the three cameras around SM2 and Table 3 gives an overview of the four camera locations.

Table 1: Mode Matching Diagnostic Sensors

Sensor	Type	Purpose	Virtual Location	Relationship with Monitored value
BSS_1	GigeCCD	IMC Beam Size	SM_1 Transmitted	Almost same as IMC beam waist
BSS_2	GigeCCD	PRM Beam Size	SM_2 Transmitted (forward)	Conjugate PRM beam size
BSS_3	GigeCCD	SM2 Beam size	SM_2 Transmitted (forward)	Indirect ROC matching
BSS_4	GigeCCD	PRM reflected	SM_2 Transmitted (backward)	Indirect ROC matching

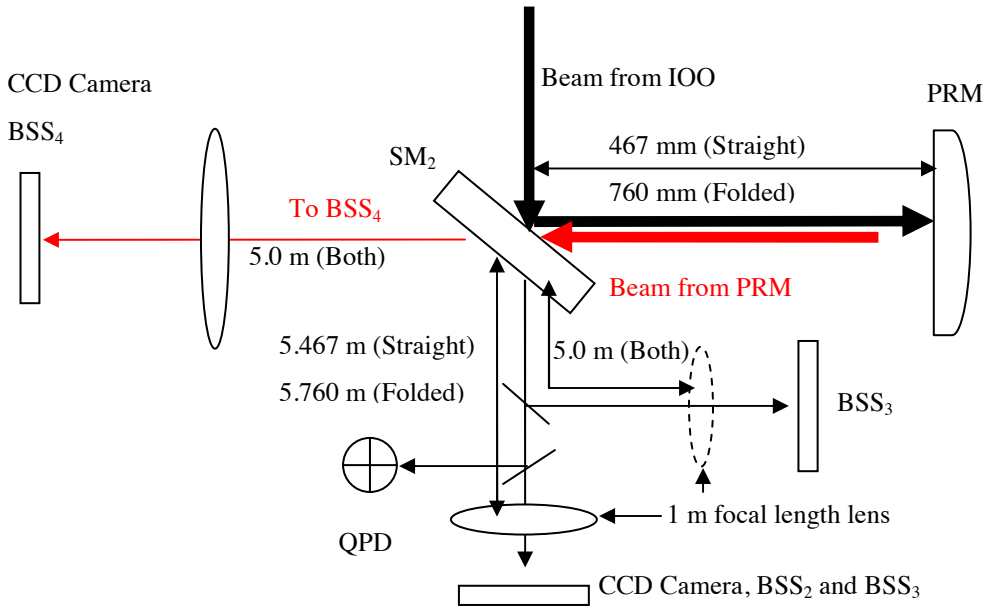

Fig. 7: Optical layout for the BSS sensors for monitoring mode matching into the interferometer.

6.2.1 BSS_1

This is a designated sensor that monitors the IMC beam size. The virtual location of this sensor is the MC waist. We relay image the beam transmitted through SM1 to ISCT1 table to BSS_1. The distance from SM1 to the bottom of the periscope is about 4 m. A 1 m lens, placed at a distance of 4 m from the MC waist, will produce an image at 1.33 m from the lens with a reduction in size of

¼. Thus a half inch camera will be sufficient to monitor this. The Rayleigh range of the IMC mode is 14 m and much larger than any uncertainties in the imaging system. The red and blue graph in Figure 8 show the measured beam size for a perfect imaging system and for an imaging system where the distance is off by 10cm. The change is much smaller than the expected change in the beam size caused by the coating absorption of 0.5 ppm in the IMC. This beam size measurement will be an essential diagnostic for the IMC to detect any abnormal behavior which could signal significant problems with the IMC absorption.

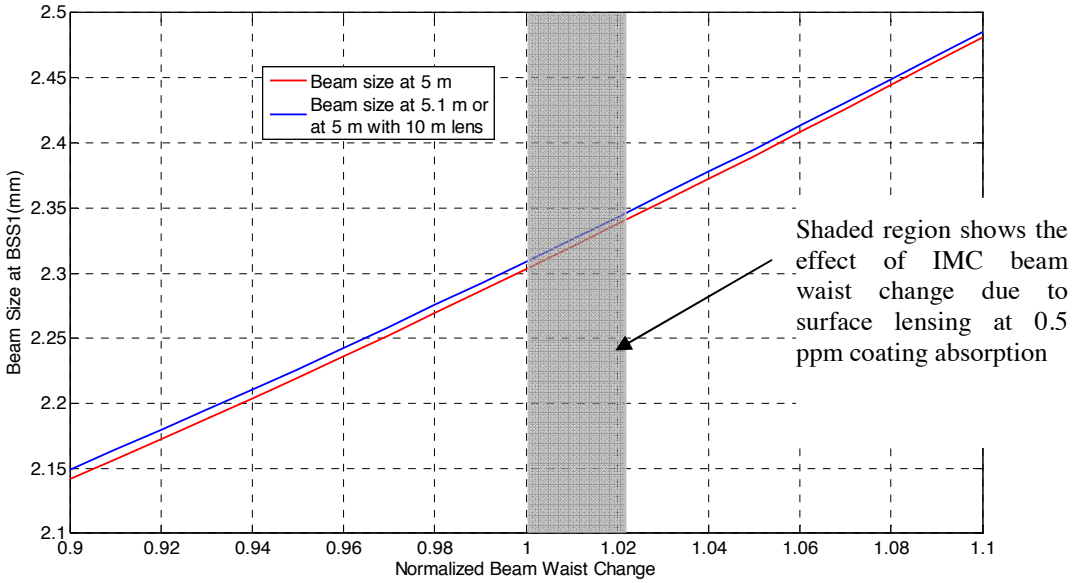

Fig. 8: Beam size measured at a camera placed 5 m away from the IMC waist. The two lines show calibration error if the camera position is incorrectly estimated by 10 cm. The shaded region corresponds to the expected change in the beam size due to MC beam waist change as a result of 0.5 pm coating absorption at full power.

6.2.2 BSS_2

BSS_2 is the sensor that monitors the beam size of the beam transmitted through SM_2. Here we relay the image of the conjugate location of the PRM located after SM_2 transmission through an imaging system. Given the location and imaging magnification of the system, we can calibrate the beam size at BSS_2 directly in terms of beam size at PRM. This will allow us to verify the IO requirement that the beam size at PRM should match the specified value. The errors in positioning the sensor are estimated in Fig. 9. The imaging system consists of a 1 m lens placed at a distance of 5 m from the conjugate location of PRM with the camera placed at 1.25 m. This forms a beam reducing telescope of 4:1. The conjugate location of the PRM HR side is 0.46670 m from SM2 HR side. Thus the position of the lens is set at 5.4667 m from SM_2 mirror.

Thus a 1 cm error produces a 6% error in the beam size at PRM. A 6% change in the beam size at PRM would create 0.3% mode mismatch. Although this number is small, we should be able to do better than 1 cm. In any case, it is evident the proposed system can measure the beam size at PRM with the required fidelity.

6.2.3 BSS_3

This sensor is very similar to BSS_2 except that instead of imaging the conjugate location of PRM, it images the beam size at SM itself in the forward direction. Thus a similar lens system is used but instead the lens is placed exactly at 5 m from the SM_2 location.

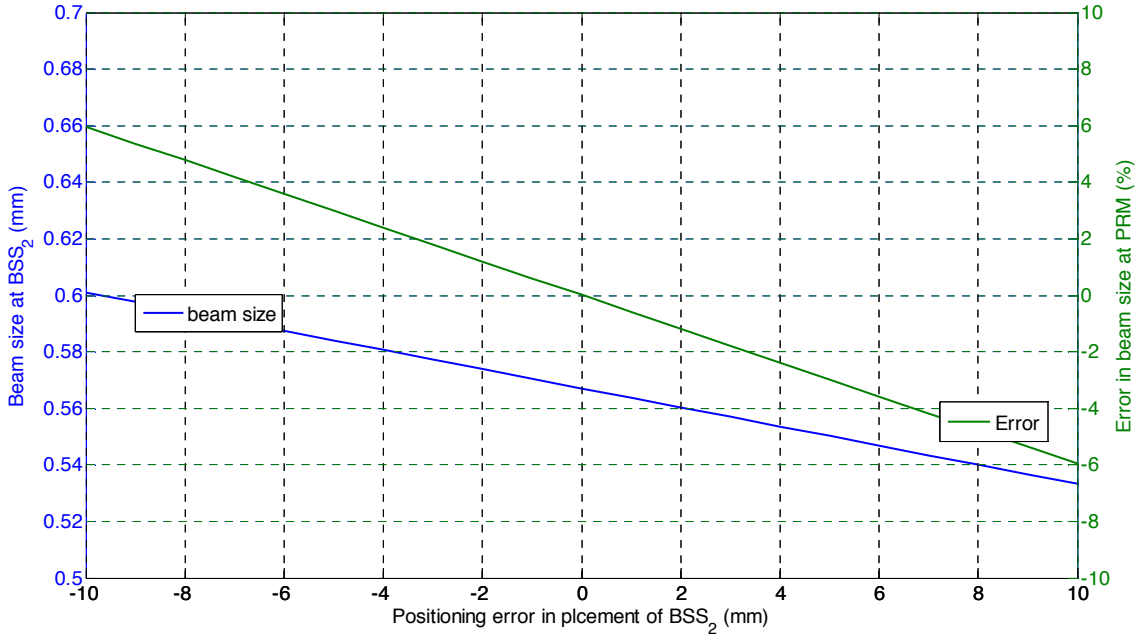

Fig. 9: Plot of beam size at BSS_2 after passing through the imaging system. The error in the calibration due to mis-positioning of the sensor (resulting in a different effective magnification) is shown on the right y-axis in green.

6.2.4 BSS_4

This sensor provides the bulk of the mode matching information. This sensor is used to image the back-reflected light from the PRM at SM_2 onto a camera. In the ideal case, when the IO beam matches the PRM ROC, the beam size at BSS_3 and BSS_4 should be exactly the same. We plan to use the same beam reducing telescope design for BSS_3 and BSS_4 thus absolute calibration of the beam size is not necessary. Note that the beam size is independently monitored at BSS_2 to determine the beam size match to the PRC.

To test the viability of measuring the beam size at BSS_4, the beam size at BSS_4 as a function of beam ROC error (plotted as Diopter (m^{-1}) in the IO is plotted in Fig. 10. Note that this is the directly reflected beam where the interferometer is not locked. The first plot shows the beam size in absolute numbers while the second plot shows the change in beam size at BSS_4 in percentage as a function of mode matching. Note that the mode matching is related to the beam ROC error as shown in Fig. 7. This figure shows that for positive beam ROC errors, the beam size increases while for negative ROC errors, the beam size would decrease. Thus a fairly well discriminating diagnostics system can be implemented even before the interferometer can be locked.

Once the interferometer of at least the PRC and short MI are locked, any mode mismatch will show up in first order as a change in the beam size and in second order in the beam shape between the locked and unlocked beams allowing to also studying the mode matching within the interferometer.

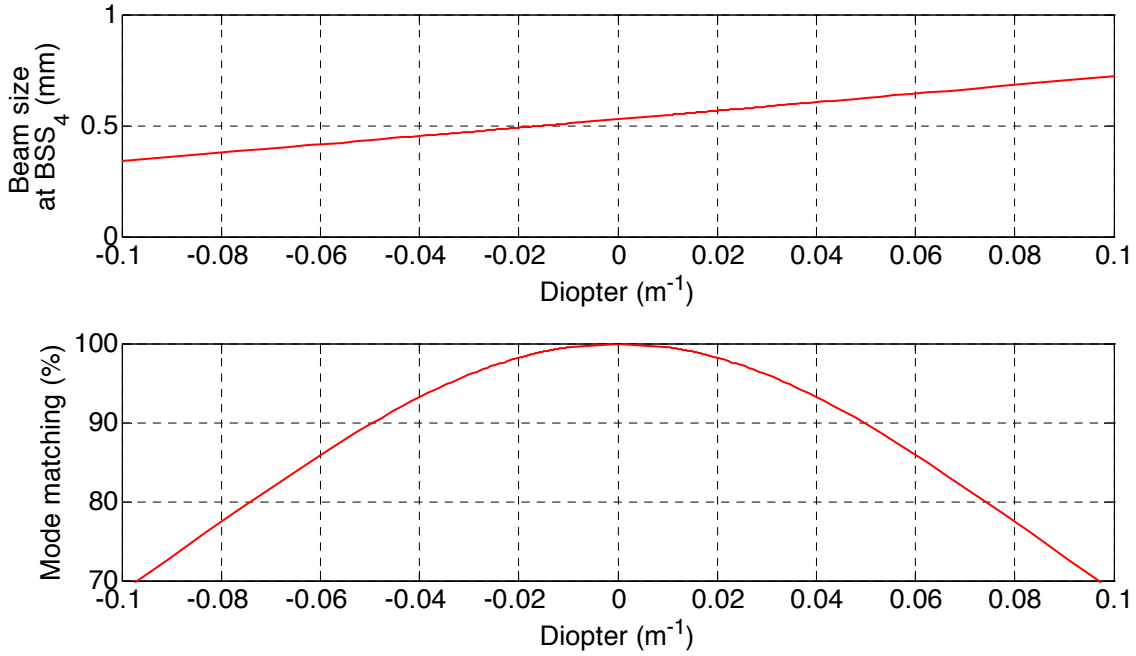

Fig. 10: Beam size values and mode matching as a function if ROC error plotted in diopters.

mbined effect of 0.5 ppm absorption of IMC mirrors (surface thermal lensing). The corresponding power loss in the mode matching is plotted on right y-axis.

6.3 Recipe for Mode matching

This section describes the installation/commissioning procedure for ensuring mode matching between IOO and PRC. This does not take into account adaptive mode matching performed via AOE. That procedure is described elsewhere.[5]

1. Monitor the beam size at BSS_1 (corresponding to 2.12 mm for straight and 2.17 mm for folded as shown in Fig. 8) to ensure that the IMC mode is not changing or is according to the specifications. The beam size should not change by more than 1% from cold to full power.
2. Monitor the beam size at BSS_2 and ensure that the beam size meets the PRC requirement. Based upon current imaging lenses and distances, a demagnification of 4 from the intended beam size at PRM is expected.

[5] M. Arain et al., "Engineering Specifications of adaptive ring heater in IOO for advanced LIGO," LIGO Technical note, LIGO-T0900407, https://dcc.ligo.org/cgi-bin/private/DocDB/ShowDocument?docid=4957

3. The beam size difference between BSS_3 and BSS_4 can be used to determine and improve the mode matching from IOO to PRC. AOE1 would be used as an actuator unless the error is so significant that a retrofit of the DKDP is needed.

7 Major mode-matching components

Table 2 shows the list of the major components needed for the mode-matching measurement. This is not an exhaustive list of IO components

Table 2: Main component to be used for Mode Matching Diagnostics

Componet	Description	Manufacturer	Part No.	Location
CCD camera	GigE camera to be used as BSS1	Prosilica	GC1380	ISCT1
CCD camera	GigE camera to be used as BSS2	Prosilica	GC1380	IOT1
CCD camera	GigE camera to be used as BSS3	Prosilica	GC1380	IOT1
CCD camera	GigE camera to be used as BSS4	Prosilica	GC1380	IOT1
BK7 Lens, F = 1.017	Imaging lens for BSS_2	CVI	PLCX-38.1-51.5-C	IOT1
BK7 Lens, F = 1.017	Imaging lens for BSS_3	CVI	PLCX-38.1-51.5-C	IOT1
BK7 Lens, F = 1.017	Imaging lens for BSS_4	CVI	PLCX-38.1-51.5-C	IOT1
50% Power Beam Splitter	Beam splitter for BSS_{2-3}	CVI	NCBS-532-100	IOT1
50% Power Beam Splitter	Beam splitter for QPD	CVI	NCBS-532-100	IOT1
Quad Photodetector	QPD for Beam steering	OSI Opto-electronics	FCI InGAAs Q3000	IOT1

8 Interface with CDS

We need the following information to be transmitted to the control room.

1. CCD Camera Interface

   We have four GigE cameras per IFO as mentioned in the bill of material in section 6. We need access to the image from these cameras in the control room and we need beam size information delivered on a designated channel.

2. QPD Signal

   We need the four channels of QPD brought in the control room and be able to manipulate them to get centering information. This would be routine task for CDS as a lot of other QPDs are being installed.

9 Summary

In summary, we have presented the pre-mode matching telescope design for advanced LIGO. We have described the sensitivity of this telescope with respect to the ROC errors; both due to mirrors' ROC errors and beam ROC errors due to thermal lensing. We have described mode matching diagnostics and operation of adaptive mode matching in advanced LIGO IOO. Interface issues and component specifications are also presented.

10 Appendix A:

Table 1: Optical Parameters and Distances in Advanced LIGO IOO

Definition	***Unit***	***PRC***	
		Straight	Folded
IMC_2 ROC	m	27.24	28.54
IMC Half Length	m	16.4731	17.2603
Beam Size at IMC_2	mm	3.378	3.458
Beam Waist inside IMC	mm	2.124	2.1738
Beam Waist inside IMC (from IMC_1 HR Side)	cm	232.5	492.5
Beam Size at IMC1 HR Side	mm	2.142	2.2
IMC Flat Mirror Substrate (n=1)	mm	73.7	73.7
Beam Waist Location outside IMC (from AR side of IMC_3)	mm	174.2	434.3 (After SM_1)
Distance b/w IMC_3 AR side and SM_1	mm	427.4	265.3
Distance between IMC Beam Waist and $PMMT_1$	m	1.5506	1.2611
ROC of $PMMT_1$	m	12.80	6.7
Beam Size at $PMMT_1$	mm	2.16	2.181
Distance between $PMMT_1$ and $PMMT_2$	m	1.1703	1.1705
ROC of $PMMT_2$	m	-6.2415	-3.1872
Beam Size at $PMMT_2$	mm	1.798	1.448
Distance between $PMMT_2$ and SM_2	m	1175.4	1.2299
Distance between SM_2 and PRM AR Side	mm	415.9	682.7
PRM ROC	m	-11	-8.87
PRM Thickness	mm	73.7	73.7
Beam Size at PRM HR Side	mm	2.24	2.08
Beam waist location from PRM (inside RC)	m	-7.1263	5.98
Beam waist after PRM	mm	1.30	1.2
Angle of Incidence at $PMMT_1$	degree	7.01	7.0
Angle of incidence at $PMMT_2$	degree	7.08	7.0

Note: Here 'Sag' is the sagitta change due to ROC while 'Tol Sag' is the change in sagitta between the nominal ROC value and when the ROC is at the end of the tolerance. For example, for IMC2, 'Tol. Sag' = (Beam size)^2/(2*27.24) - (Beam size)^2/{2*(27.24+0.03)}

Table 2: Component Parameters for Recycling Cavity Mirrors

Optics	ROC (m)		Beam Size (mm)		Sag (μm)		ROC Tolerance in % and mm			Tol. Sag (nm)	
	Straight	Folded	Straight	Folded	Straight	Folded	Both (%)	Straight (mm)	Folded (mm)	Straight	Folded
IMC1	Inf	Inf	2.1	2.2	0.00	0.00	0.1	80E6	80E6	0.03	0.03
IMC2	27.24	28.54	3.4	3.5	0.21	0.21	0.1	30.0	31.4	0.2	0.2
IMC3	Inf	Inf	2.1	2.2	0.00	0.00	0.1	80E6	80E6	0.01	0.01
PMMT1	12.80	6.7	2.2	2.2	0.18	0.36	1	128.0	66.7	1.8	3.5
PMMT2	-6.24	-3.18	1.8	1.45	-0.26	-0.33	1	-62.4	-31.8	-2.6	-3.2